IRAQI JOURNAL OF APPLIED PHYSICS
Vol. 22, No. 3, July-September 2026, pp. 350-357

Qasim S. Kareem [1*]
Nadhim A. Abdullah [2]
Hassan K. Ibrahim [3]
Khalid I. Ajeel [4]
Hussein F. Hussein [3]
Ibrahim K. Ibrahim [5]

Structural and Optical Characteristics of ZnO Nanoparticles-Doped Epoxy Resin Thin Films

In this study, pure epoxy resin (ER) was doped with zinc oxide nanoparticles (ZnONPs) at different weight fractions (0.01, 0.03, 0.05, 0.07 and 0.09 wt.%). The chemical cast deposition method was used to make six thin film samples (one pure and five doped). The structural and the linear optical properties of the prepared samples were investigated via X-ray diffraction (XRD) and UV-visible spectroscopy. The absorbance and reflectance have increased with increasing ZnONPs doping weight fraction, while transmittance has decreased and the energy bandgap have decreased from 3.42 to 2.79 eV. An increase in Urbach energy from 0.09 to 0.60 eV was observed with increasing doping weight fraction. Results presented herein revealed that the structural and optical properties of epoxy resin were improved by doping with ZnO nanoparticles.

Keywords: Epoxy resin; Zinc oxide; Thin films; Nanocomposites
Received: 26 May 2025; Revised: 16 November; Accepted: 23 November; Published: 1 July 2026

[1] Department of Physics, College of Education, University of Al-Qadisiyah, Diwaniyah, IRAQ
[2] Department of Materials Science, Polymer Research Centre, University of Basrah, Basrah, IRAQ
[3] Physics Department, College of Education for Pure Science, University of Basrah, Basrah, IRAQ
[4] Medical Instrumentation Techniques Engineering Department, Al-Kunooze University, Basrah, IRAQ
[5] Department of Chemistry and Polymer Technology, Polymer Research Center, University of Basrah, Basrah, IRAQ
* Corresponding author email: qasim.alshook@qu.edu.iq

1. Introduction

Epoxy resins are typically prepared by the interaction among bisphenol and 2-(Chloromethyl) oxirane [1]. Epoxy resins indicates to both the prepolymer and the resin or hardener method used to cure it. The development of highly oriented and transparent ZnO nanocomposites has been the subject of extensive research in recent years due to its many uses in technological devices, biosensors, and photo detectors [2-5]. They have exhibited markedly better physical properties, compared with the pure epoxy resin [2,3]. Recently, nanoparticles have got a lot of interest due to their outstanding features in various materials and their applications systems such as ZnO nanoparticles, which are n-type semiconductor with a fixed wurtzite structure and a wide band gap. Unlike many of its competitors, ZnO is inexpensive abundant, chemically stable and non-toxic [4,5]. In this study, the epoxy:ZnONPs nanocomposites were fabricated by mixing ZnO NPs with epoxy resin at different weight fractions of ZnO nanoparticles. The optical properties of these nanocomposites were studied as functions of the ZnO NPs doping weight ratio (0.01, 0.03, 0.05, 0.07, and 0.09 wt.%) at room temperature in UV-visible regions.

2. Experimental Work

An epoxy resin (Shape of product: 136-2A, and part number: 20209150) was mixed at a ratio of (3:1) to hardener was used in this work. Zinc oxide nanoparticles (ZnONPs) were provided by SkySpring nanomaterials Inc., USA, with 99.8% purity, 10-30nm size, product no. 8410DL, were used as doping material in this study. A three-steps solvent cleaning processes by ultrasonic bath technique were done on the glass substrates with dimensions of 75x25x1mm. They were acetone for 5 min., isopropyl alcohol for 5 min., deionized water for 5 min., followed by two hours drying at 80°C in an oven. The ER/ZnONPs mixtures were prepared by adding a specific amounts of ZnO NPs (0.001, 0.003, 0.005, 0.007 and 0.009 g), as shown in table (1), in a multistep process. Firstly, mechanical mixing of 10 g of epoxy resin with a definite quantity of ZnO NPs for two minutes, and secondly, the mixture was sonicated for 15 min in order to produce as high as much dispersion of ZnO NPs into epoxy matrix. However, the third step involved mixing epoxy with hardener at ratio of 3:1. Cast deposition method at room temperature was used to make the samples, then they were left at room temperature to dry for two days to ensure the best curing. The thickness of each sample was measured by digital micrometer, as shown in table (2).

The X-ray diffraction (XRD) was carried out using Philips PW 1700 X'Pert Pro diffractometer, anode of CuK X-ray source, anode current of 40 mA and operating voltage of 45 kV (Leiden, Netherlands), with 2θ varying between 10° and 80° in continuous style, with a step size of 0.02°, in 0.35 s per step for a count time.

Table (1) The weights, weight fractions of pure and ZnONPs-doped ER composite samples prepared in this work

Sample	Epoxy Resin (ER) (g)	Epoxy resin (ER) (wt.%)	ZnO-NPs (g)	ZnO-NPs (wt.%)
S_0	10	100	0	0
S_1	10	99.99	0.001	0.01
S_2	10	99.97	0.003	0.03
S_3	10	99.95	0.005	0.05
S_4	10	99.93	0.007	0.07
S_5	10	99.91	0.009	0.09

Table (2) The thickness of pure and ZnONPs-doped ER composite samples prepared in this work

Sample	Description	Thickness (mm)
S_0	Pure (ER)	0.435
S_1	ER/ZnO NPs 0.01%	0.542
S_2	ER/ZnO NPs 0.03%	0.556
S_3	ER/ZnO NPs 0.05%	0.497
S_4	ER/ZnO NPs 0.07%	0.563
S_5	ER/ZnO NPs 0.09%	0.566

3. Results and Discussion

The XRD measurements were performed via the Bragg's diffraction law and the average crystallite size (D_{hkl}) calculated according to Debye-Scherer formula as [6]:

$$2d_{(hkl)}sin\theta = n\lambda \quad (1)$$

$$D_{(hkl)} = \frac{K\lambda}{\beta cos\theta} \quad (2)$$

The optical properties of prepared samples were determined by SHIMADZU 1800 UV-VIS spectrophotometer (Japan) in spectral range of 300-900 nm. The absorbance (A) can be determined by [7]:

$$A = -LogT = -Log\left(\frac{I}{I_0}\right) = Log\left(\frac{I_0}{I}\right) \quad (3)$$

where I_0 is the incident intensity of light, I is the intensity of the absorbed light, and T is the transmittance [8], which can be estimated from [9]

$$T = 10^{-A} \quad (4)$$

The following relationship can be used to estimate the reflectance (R) based on the refractive index amount as [10]

$$R = \frac{(n-1)^2+k^2}{(n+1)^2+k^2} \quad (5)$$

The reflectance can also be obtained from the rule of keep of energy as [11]

$$R + T + A = 1 \quad (6)$$

The absorption coefficient (α) is expressed via Lambert-Beer's law as [12]

$$I = I_0 e^{-\alpha t} \quad (7)$$

$$\alpha = \frac{2.303}{t} exp\left(\frac{I_0}{I}\right) = \frac{2.303}{t} A \quad (8)$$

where t is the sample thickness

Extinction coefficient (k) means the imaginary amount of complex refractive index (n^*) as [13]

$$n^* = n - ik \quad (9)$$

where k is determined by [14]

$$k = \frac{\alpha\lambda}{4\pi} \quad (10)$$

Refractive index (n) is the ration of light speed in vacuum (c) to its speed in a medium (v) as [15]

$$n = \frac{c}{v} \quad (11)$$

The refractive index can also be determined by [16]

$$n = \sqrt{\frac{4R}{(1-R)^2}} - k^2 + \frac{1+R}{1-R} \quad (12)$$

The dielectric constant (ε) of a composite material contains two parts. These parts are known as real (ε_r) and imaginary (ε_i), where [17]

$$\varepsilon = \varepsilon_r + i\varepsilon_i \quad (13)$$

where [18]

$$\varepsilon_r = n^2 + k^2 \quad (14)$$

$$\varepsilon_i = 2nk^2 \quad (15)$$

Optical conductivity ($\sigma_{op.}$) can be expressed as [19]

$$\sigma_{op} = \frac{\alpha nc}{4\pi} \quad (16)$$

The photon absorption in many materials is described by Tauc's relation as [20]

$$\alpha h\nu = B\left(h\nu - E_g\right)^r \quad (17)$$

where E_g is the optical band gap, B is a constant, h is Planck's constant, ν is the frequency of radiation, r is order of the optical transition determined via electronic transition [21]

Supposing that the value of α close to the band side exhibits an exponential reliance on photon energy, as [22]

$$\alpha = \alpha_0 exp\left(\frac{h\nu}{E_U}\right) \quad (18)$$

where α_0 is a constant, E_U is Urbach energy, and $h\nu$ is photon energy

4. Results and Discussion

Figure (1) illustrates the XRD patterns for both the pure epoxy (black line), and the doped epoxy with a different concentrations of ZnONPs (colored lines). The amorphous structure of pure epoxy was verified with the presence of two peaks; the first at 2θ=18.6°, with a broad range between 10°-30°, and the second peak at 2θ=44° with a broad range between 37.5° and 50° [23]. In case of ZnO nanoparticles in the epoxy matrix; basically, semi-crystalline structure is seen for samples S_1, S_3, and S_5, but there was a slightly shift in the peak at 18.6° with decreased amplitude, while the second peak was disappeared in XRD pattern of doped ER comparing to pure ER as an effect of doping because due to the incorporation of ZnONPs into epoxy chains in the interlayer spacing of prepared samples [24].

The UV-visible absorption spectra of the pure epoxy resin (ER) and doped with ZnO nanoparticles (ER/ZnONPs) nanocomposites at different weights doping ratios of ZnO NPs (0.01, 0.03, 0.05, 0.07 and 0.009 wt.%) at room temperature were depicted in Fig. (2a). The absorbance (A) increases with increasing weight fraction of ZnONPs with respect to the pure epoxy resin (ER). As well, a red shift in the absorption peaks was observed for ZnONPs-doped ER

when compared to pure epoxy resin (ER) due to the initial excitation electronic transitions occurring in ER/ZnONPs nanocomposite. However, the optical absorption of ER/ZnONPs nanocomposites displays a wide peak due to n–π* (HOMO–LUMO) transitions. A variation in composite structure is shown by the formation of new and wide peaks when the weight fraction of ZnO NPs is increased [25]. Also, the reaction of pure ER with ZnO NPs could result in the peak shift and it indicates a decrease in the bandgap of ER/ZnONPs nanocomposite. However, absorption peak for pure epoxy resin (ER) occurs in UV region and exactly at 362 nm with energy gap of 3.42 eV. This agrees with previous results in reference [26].

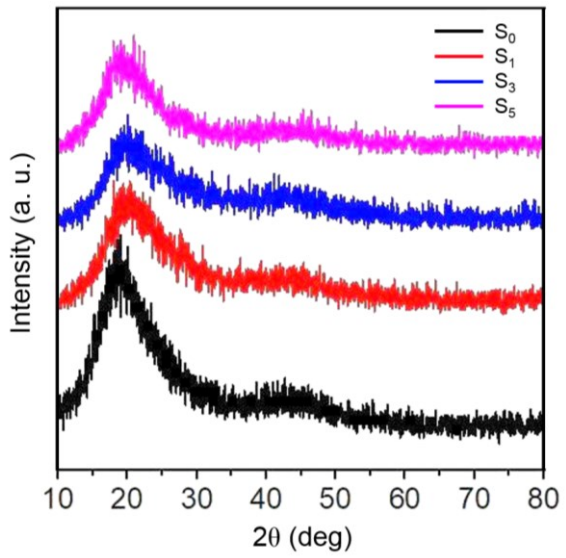

Fig. (1) XRD patterns of pure ER and ZnONPs-doped ER

The different weight fractions of ZnO NPs added to the pure epoxy resin (ER) create new defects (new polaron levels) within the direct optical energy gap for ER. These defects increase with increasing ZnO NPs loading, which help moving electrons from valence band (VB) to conduction band (CB) (i.e., translating electrons from HOMO to LUMO). On the other hand, when the surface area of nanoparticles is high, it creates new localized states because too many atoms on the surface can be available for interaction with dopants. This leads to increase their chemical reactivity on the surface compared with the material's bulk. Figure (2) makes it apparent that all pure and doped ER nanocomposites showed decreasing absorbance with increasing wavelength, whereas the absorbance increased as ZnO NPs weight ratios was increased. The number of particles that absorb incident light energy via free electrons increases as their weight ratio is increased as confirmed by the literature [27]. The experimental results indicated that the best linear optical properties (e.g., absorption coefficient α) was observed for ER sample doped with 0.09 wt.% ZnO NPs and thickness of 0.566 mm. Furthermore, the film thickness can influence its crystalline structure, defect density, and bandgap energy, all of which can impact the absorption coefficient. For example, a change in energy bandgap with thickness can alter the mechanism of photon absorption.

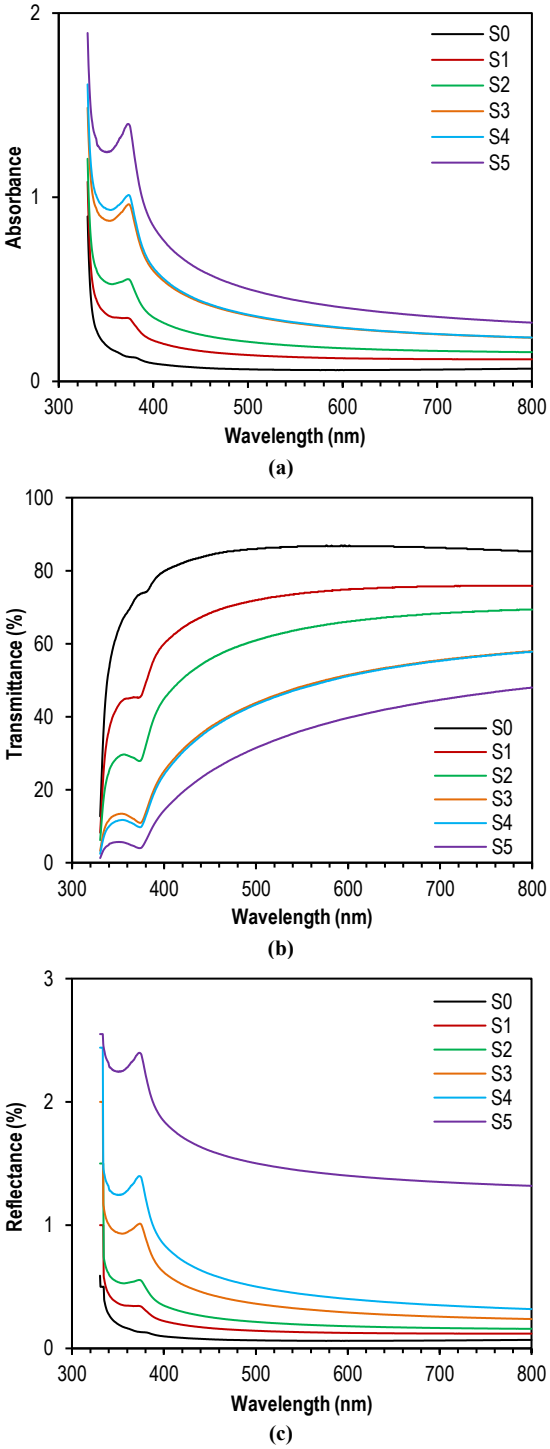

Fig. (2) (a) Absorption spectra, (b) transmission spectra, and (c) reflectance vs. wavelength for pure and ZnONPs-doped ER

The transmittance (T) of the pure and doped ER composites with varying doping ratios (0.01, 0.03, 0.05, 0.07 and 0.09 wt.%) of ZnO NPs as a function of wavelength at room temperature are displayed in Fig. (2b). It illustrates how the transmittance increases with wavelength and when the doping ratio of ZnONPs is increased, the transmittance decreases. The results imply that the doping ratio of ZnONPs is the main reason behind decreasing transmittance. This effect can be explained via the fact that increasing doping ratio increased the number of localized levels, which in turn reduced transmittance, in agreement with reference [28]. Figure (2c) refers to variation of the reflectance (R) with wavelength for all samples. The reflectance exhibits similar behavior of that of the absorbance. Physical factors that affect material's reflectance include its surface properties, composition, and the characteristics of the incident light. The reflectance increases with increasing ZnONPs weight ratio as this may create flaws in the pure epoxy resin (ER), which enhances or increase ray scattering and reflection. This is agreement with previous results [29].

Figure (3) indicates the variation of absorption coefficient (α) with wavelength for the prepared samples. It was found that the value of α for pure and doped epoxy resin nanocomposites are higher than 10^4 cm^{-1} in the visible region, which means that the prepared samples have allowed direct energy bandgap. So that the r value in Eq. (17) is equal to 0.5. Moreover, the value of α decreases with increasing wavelength, whereas it increases with increasing the weight ratios of ZnO NPs (0.01, 0.03, 0.05, 0.07 and 0.09 wt.%) due to the decrease in energy bandgap with increasing weight ratio of ZnO NPs as the number of localized levels is increased. Similar results were reported in literature [30].

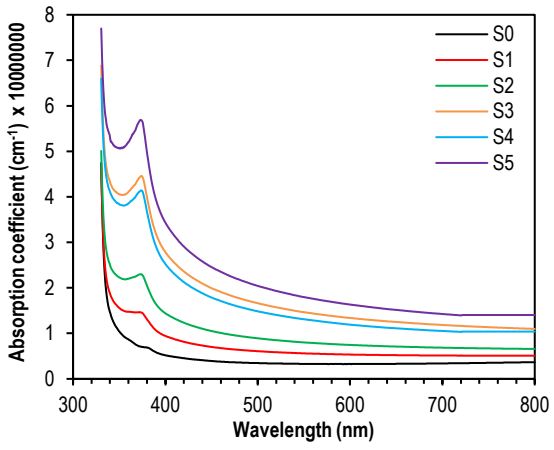

Fig. (3) Variation of absorption coefficient with wavelength for pure and ZnONPs-doped ER composites

Figure (4) shows the variation of the extinction coefficient (k) with wavelength for different weights ratios (0.01, 0.03, 0.05, 0.07 and 0.09 wt.%) of ZnO NPs in epoxy resin (ER). It is clear that the extinction coefficient decreases with increasing wavelength for all prepared samples. On the other hand, the extinction coefficient increases as the weight ratio of ZnONPs is increased. This variation could be explained as the high value of absorption coefficient reveals an increase in the incident light absorption since the optical energy gap decreases as ZnONPs weight ratio is increased. The behavior of the extinction coefficient (k) is similar to that of the absorption coefficient (α), which agrees with previous results [31].

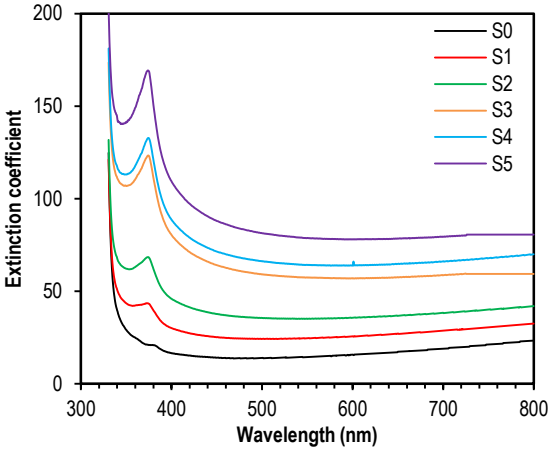

Fig. (4) Variation of extinction coefficient with wavelength for pure and ZnONPs-doped ER composites

Figure (5a) shows the variation of the refractive coefficient (n) with wavelength for pure ER and ZnONPs-doped ER nanocomposite samples according to Eq. (12). It is found that the values of n decreases with increasing wavelength (i.e., decreasing photon energy). However, values of n for epoxy resin/ZnONPs composites increase with increasing weight ratio of ZnONPs. Furthermore, figure (5b) shows that the value of n increases with increasing the weight ratio of ZnONPs for all prepared samples, as shown table (3). This behavior may be attributed to the increase in reflection, which in turn affects the refractive index, i.e., this behavior can be explained by the decrease in the light velocity through the sample when its refractive index increases. Pure and doped ER thin films depend on the surface topography of polymeric nano films, with an increase in surface topography at varied weight doping proportions (0.01, 0.03, 0.05, 0.07 and 0.09 wt.%) from ZnONPs, *n* is increasing. The figure makes it evident that as the incoming photon energy increases, the values of *n* rise in accordance with the rise in the absorption coefficient α_a (cm^{-1}) and the extinction coefficient (k), similar results are reported in literature [32].

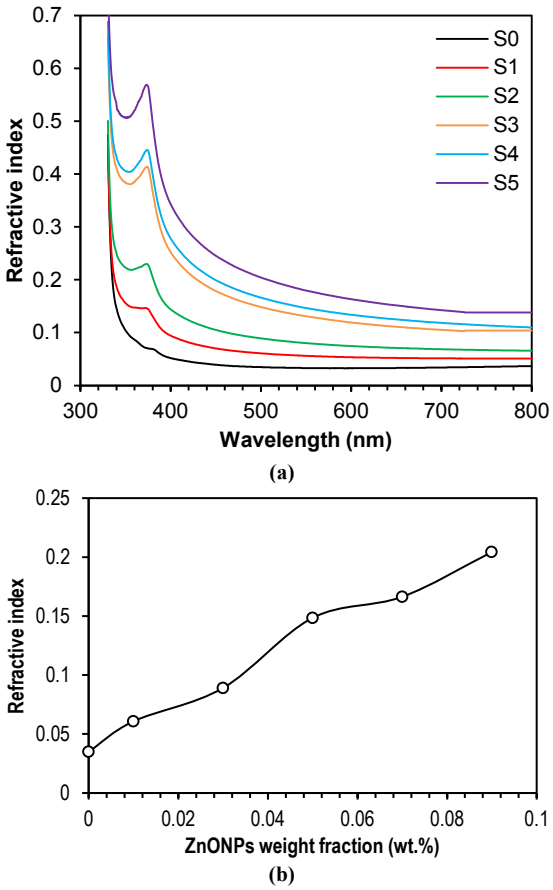

Fig. (5) Variation of refractive index with wavelength for the prepared samples at 500 nm

Table (3) Refractive index values for pure and ZnONPs-doped doped ER composite samples

Sample	Refractive index (n)
Pure (ER)	0.0349421
ER/ZnO NPs 0.01%	0.0607618
ER/ZnO NPs 0.03%	0.0890549
ER/ZnO NPs 0.05%	0.1484883
ER/ZnO NPs 0.07%	0.1663535
ER/ZnO NPs 0.09%	0.204259

Variations of the real (ε_r) and imaginary (ε_i) parts of the dielectric constant with wavelength for pure and ZnONPs-doped ER composite samples in the spectral range of 300-900 nm are shown in Fig. (6). The differences between ε_r and ε_i is due to the changes in the reflectance (R) and absorbance (A). It is evident that the nature of the real part (ε_r) is comparable to that of the refractive index (n), whereas the imaginary part (ε_i) depends on the extinction coefficient (k) values and absorption coefficient (α). Compared to the imaginary part, the real part is higher. These results agree with previous results [33].

According to Eq. (16), figure (7) shows the variation of the optical conductivity (σ_{op}) for prepared samples, where the optical conductivity decreases with increasing wavelength due to the decrease in the absorption coefficient and the refractive index. On the other hand, the optical conductivity increases with increasing ZnO NPs weight fraction. This result could be attributed to the enhanced electron transition between the conduction and valence bands, as a result of creating new energy states because the energy bandgap got narrower. This result is in agreement with previous results [34].

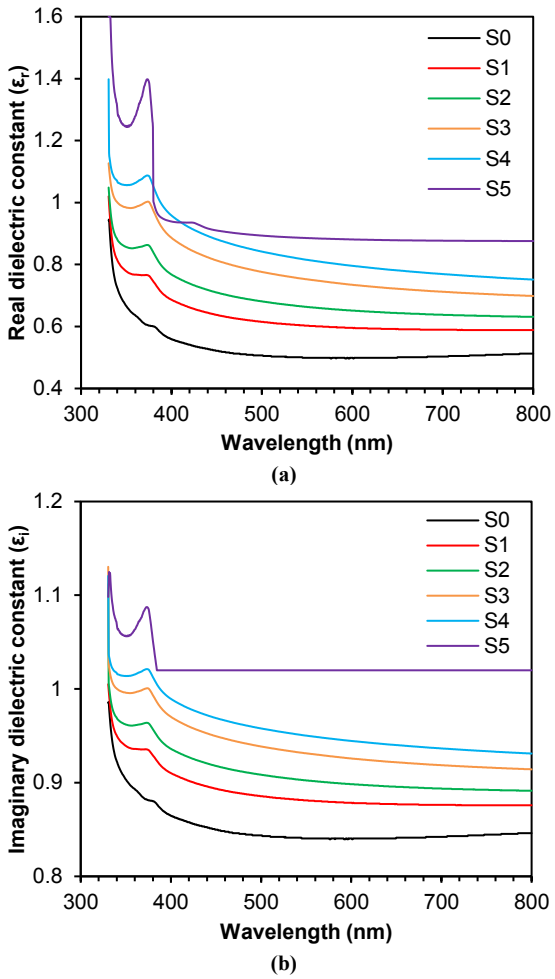

Fig. (6) Variation of (a) real dielectric constant (ε_r) and (b) imaginary dielectric constant (ε_i), with wavelength for pure and ZnONPs-doped ER composites

As mentioned before, the values of the absorption coefficient (α) for all prepared nanocomposites are $>10^4$ cm^{-1}, so, the prepared samples have allowed direct energy bandgap, which was determined by Tauc's plots. The linear part of the curve is extrapolated to intersect the horizontal ($h\nu$) axis at $(\alpha h\upsilon)^2$ equal to zero to get the value of E_g, as shown in Fig. (8) and table (4).

Figure (9) illustrates the variation of the allowed direct (E_g) with the weight ratio of ZnO NPs in the prepared nanocomposites, as it decreases with increasing the ZnO NPs weight ratio due to new energy states created within the bandgap, and hence, facilitate electron transition from the valence band (VB) to the conduction band (CB). Thus, the band gap

decreases [35] in agreement with previous results [36]. The Urbach energy tails (E_U) were calculated from the slope of the straight line of plotting against hυ. Figure (10) displays the variation of ln(α) with $h\nu$ for the prepared nanocomposites. From table (2), E_U is ranging through 0.09-0.60 eV. The variation of E_U with increasing weight ratio of ZnO NPs is shown in Fig. (11). In general, the concentration of nanoparticles affects the degree of disorder in the nanocomposite sample and may cause damage to the structure since the nanoparticles act as an external source of disorder and their effects become more pronounced as more particles are incorporated into the structure.

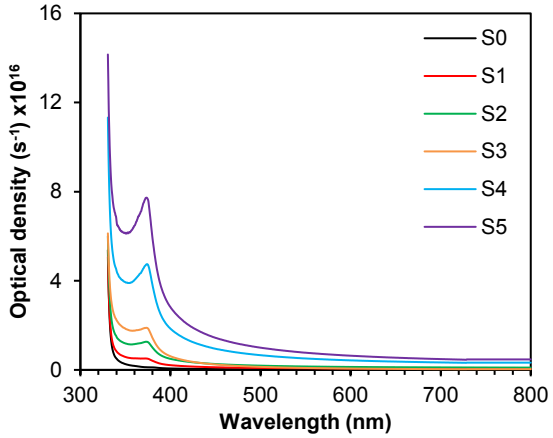

Fig. (7) Variation of optical conductivity with wavelength for pure and ZnONPs-doped ER composites

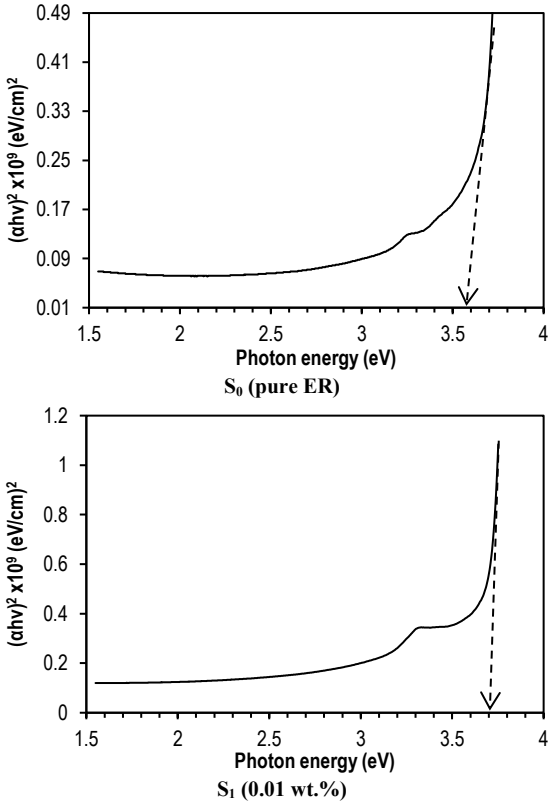

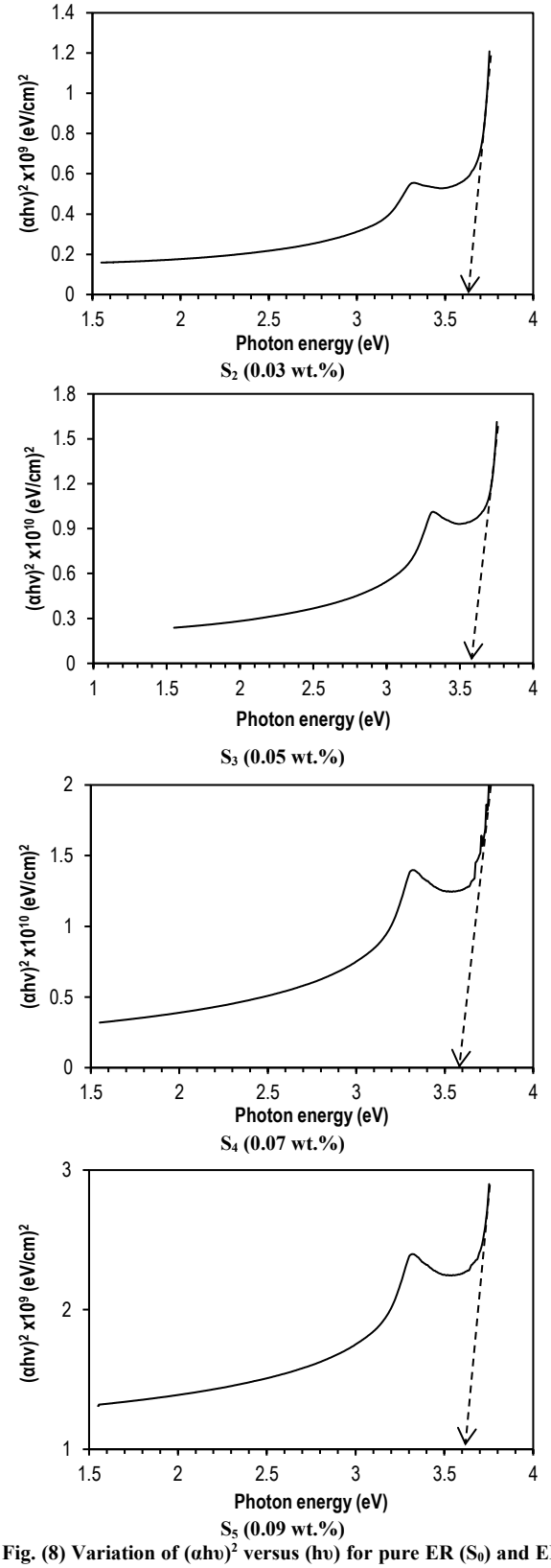

Fig. (8) Variation of $(\alpha h\upsilon)^2$ versus (hυ) for pure ER (S_0) and ER doped with different weight ratios of ZnONPs

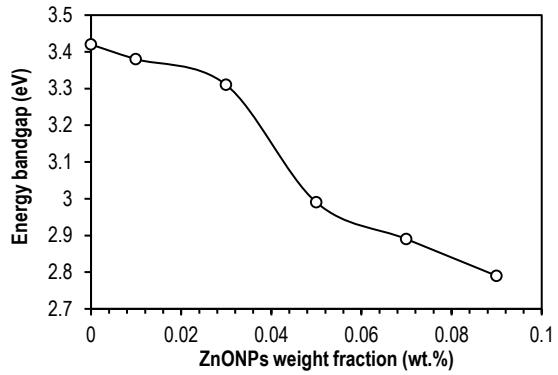

Fig. (9) Variation of energy bandgap (E_g) versus doping weight ratio of ZnO NPs in ER composites

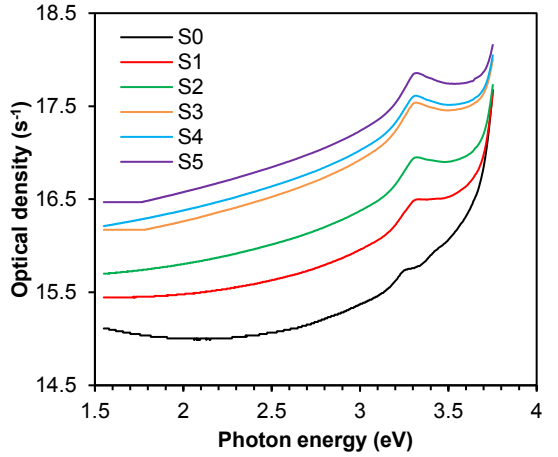

Fig. (10) Plots of ln(α) versus hv for pure and ZnONPs-doped ER composites

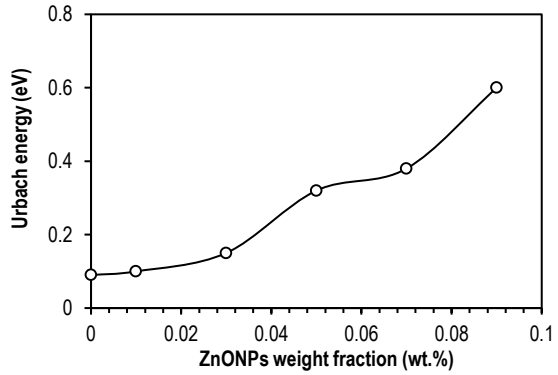

Fig. (11) Variation of E_U versus doping weight ratio for pure and ZnONPs-doped ER composites

Table (4) Values of E_g and E_U for pure and ZnONPs-doped ER composites

Sample	Description	E_g (eV)	E_U (eV)
S_0	Pure (ER)	3.42	0.09
S_1	ER/ZnO NPs 0.01%	3.38	0.10
S_2	ER/ZnO NPs 0.03%	3.31	0.15
S_3	ER/ZnO NPs 0.05%	2.99	0.32
S_4	ER/ZnO NPs 0.07%	2.89	0.38
S_5	ER/ZnO NPs 0.09%	2.79	0.60

5. Conclusions

It is found that the structural and optical properties of epoxy resin (ER) as a result of doping with ZnO NPs. Semi-crystalline structure of ZnONPs-doped ER nanocomposites was revealed. A redshift in the direct allowed energy bandgap (Eg) of the nanocomposites was observed due to doping with ZnO NPs. The absorption peak for pure ER occurs in UV region at 362 nm and E_g of 3.42 eV, which is larger than that of ZnONPs-doped ER nanocomposites. The structural and optical properties of the ER were enhanced due to doping with ZnO NPs to serve many applications such as nanocomposite coatings, optics and electronics.

References

[1] M.S.S. Al-Salimi1, W.R.N. Ali and K.M. Habeb, "Optical and dielectric properties of epoxy resin filled with titanium dioxide properties", *Electron. J. Univ. Aden Basic Appl. Sci.*, 4(2) (2023) 147-154.

[2] S. Hardon et al., "The Influence of ZnO Nanoparticles on the Dielectric Properties of Epoxy Resin", *AIP Conf. Proc*., 2131(1) (2019) 020015.

[3] A. Miravete, "The Effect of Nanosized Filler on Electrical Performance of Epoxy Resin", PhD thesis, University of Southampton, UK (2012).

[4] O.A. Hammadi, "Fluorescence Characteristics of Random Gain Media Fabricated from Fluorescein Dye Containing Zinc Oxide Nanoparticles in Transparent Organic Hosts", *Iraqi J. Mater.,* 5(1) (2026) 47-52.

[5] M.J. Jawad, Z.K. Alobad and A.S. Hasan, "Effect of (ZnO) Nanoparticles on The Mechanical, Antibacterial and Morphological Properties of Epoxy Resin", *Adv. Mech*., 9(3) (2021) 41-48.

[6] A.K. Singh, **"Advanced X-ray Techniques in Research and Industry"**, IOS Press (US 2005).

[7] K.I. Ajeel and Q.S. Kareem, "Synthesis and characteristics of Polyaniline (PANI) Filled by Graphene (GR) Nano film", *IOP Conf. Ser. J. Phys*., 1234 (2019) 012020.

[8] E.F.H. Brittain, W.O. George and C.H.J. Wells, **"Introduction to Molecular Spectroscopy: Theory and Experiment"**, Academic Press, (NY, 1970).

[9] K.I. Ajeel and Q.S. Kareem, "Preparation of (polyaniline/graphene) composite thin films for gas sensing application", PhD thesis, University of Basrah, Iraq (2021).

[10] K. Gupta, P.C. Jana and A.K. Meikap, "Optical and Electrical Transport Properties of Polyaniline-Silver Nanocomposite", *Synth. Met*., 160(13) (2010) 1566-1573.

[11] C. Mwolfe, N. Holouyak and G. Stillman, **"Physical Properties of Semiconducter"**, Prentice Hall, (NY, 1989).

[12] R.K.F. Alfahed et al., "Spectroscopic ellipsometry study and variability of optical parameters for blend polymer (PVA:POT) thin films", *Proceed. First Int. Third Sci. Conf., College of Science, University of Tikrit, Iraq (2018)*.

[13] K.I. Ajeel and Q.S. Kareem, "Optical properties for prepared Polyaniline/Graphene nano composites films", *J. Basrah Res.: Sci.,* 45(2) (2019) 162-177.

[14] G. Ding et al., "Thickness and microstructure effects in the optical and electrical properties of silver thin films", *AIP Adv*., 5(11) (2015) 117234.

[15] M. Born and E. Wolf , **"Principles of Optics: Electromagnetic Theory of Propagation, Interference and Diffraction of Light"**, 7th ed., Cambridge University Press (1999).

[16] M.A. Aziz., M.A. El-Sherbini and M.A. El-Dessoky, "Refractive index of epoxy grafted with different percentages of titanium dioxide", *J. Appl. Polym. Sci.,* 135(37) (2017) 42-47.

[17] J.H. Nahida and R.F. Marwa, "Study of the Optical Constants of the PMMA/PC Blends", *Eng. Technol. J.*, 29(4) (2011) 585-595.

[18] T.K. Hamad, "Refractive Index Dispersion and Analysis of the Optical Parameters of (PMMA/PVA) Thin Film", *J. Al-Nahrain Univ*., 16(3) (2013) 164-170.

[19] Z.U. Abdin et al., "Effect of Fe dopant on physical properties of antimony sulphide (Sb_2S_3) thin films", *Chalcogen. Lett*., 16(1) (2019) 37-48.

[20] P.R. Jubu et al., "Dispensability of the conventional Tauc's plot for accurate bandgap determination from UV–vis optical diffuse reflectance data", *Result. Opt.,* 9 (2022) 100273.

[21] A. Umar et al., "Enhanced photocatalytic degradation of harmful dye and phenyl hydrazine chemical sensing using ZnO nanourchins", *Chem. Eng. J*., 262 (2015) 588.

[22] C. Zaouche et al., "The determination of Urbach energy and optical gap energy by many methods for Zn doped NiO thin films fabricant semiconductor by spray pyrolysis", *Digest J. Nanomater. Biostruct*., 17(4) (2022) 453-1461.

[23] J. Tian et al., "The correlated effects of filler loading on the curing reaction and mechanical properties of graphene oxide reinforced epoxy nanocomposites", *J. Mater. Sci*., 56(5) (2021) 3723-3737.

[24] K. Mahmoud and O.L. Tashlykov, "Synthesis of a new epoxy resin reinforced by ZnO nanoparticles for γ-ray shielding purposes: Experimental and Monte Carlo simulation assessments", *Radiat. Phys. Chem*., 208 (2023) 110938.

[25] S.K. Das, S. Paul and S. De, "Effect of TiO_2 nanoparticles on the optical and thermal properties of epoxy resin", *J. Mater. Sci. Eng.,* 4(2) (2016) 1-7.

[26] M. Akter, H. Ozdemir and K. Bilisik, "Epoxy/Graphene Nanoplatelet (GNP) Nanocomposites: An Experimental Study on Tensile, Compressive, and Thermal Properties", *Polymers,* 16(11) (2024) 1483.

[27] A. Mehto et al., "Preparation and Characterization of Polyaniline/ZnO Composite Sensor", *J. Nanomed. Res.,* 5(1) (2017) 1-8.

[28] D. Dhanapal et al., "Fabrication of tetra glycidyl epoxy nanocomposites functionalized with amine-terminated zinc oxide with improved mechanical and thermal properties", *J. Mater. Res. Technol.,* 21 (2022) 3947–3960.

[29] M.A. Alam et al., "Effects of SiO_2 and ZnO nanoparticles on epoxy coatings and its performance investigation using thermal and nanoindentation technique", *Polymers,*13(9) (2021) 1490.

[30] S. Moussa, F. Namouchi and H. Guermazi, "Elaboration, structural and optical investigations of ZnO/epoxy nanocomposites", *Euro. Phys. J. Plus,* 130 (2015) 152.

[31] H. Durmus, "Optical properties of modified Epoxy resin with various oxime derivative in the UV-Vis spectra region", *J. Appl. Polym. Sci.,* 120, (2010) 1490-1495.

[32] A. Bouzidi et al., "Effect of the different concentrations of ZnO:Mn incorporation on the microstructure and dielectric properties of epoxy nanocomposites", *J. Mater. Sci.: Mater. Electron.,* 29(7) (2018) 5908–5917.

[33] Š. Hardoň et al., "The Influence of ZnO nanoparticles in the epoxy resin on the complex permittivity and dissipation factor", *Transport. Res. Procedia.,* 40 (2019) 30–33.

[34] A. Abdel-Galil, H.E. Ali and M.R. Balboul, "Nano-ZnO Doping Induced Changes in Structure, Mechanical and Optical Properties of PVA Films", *Arab J. Nucl. Sci. Appl.,* 48(2) (2015) 77-89.

[35] M. Yuan et al., "Fabrication of cyclodextrin modified graphene oxide nanocontainers loading zinc ion and its application in water-based epoxy resin coatings", *Colloids Surf. A: Physicochem. Eng. Aspects*, 726(2) (2025) 137679.

[36] I. Fayaz and G.M. Peerzada, "Synthesis of multifunctional metalloresins and evaluating the effect of zinc oxide nanoparticles on mechanical, adhesion and flame-retardant properties of epoxy resins", *J. Mole. Struct.*, 1326 (2025) 141077.

